

Phonon dispersion curves of two-dimensional colloidal crystals: on the wavelength dependence of friction

J. Baumgartl,¹ J. Dietrich,¹ J. Dobnikar,² C. Bechinger,^{1,3} and H.H. von Grünberg⁴

¹*Physikalisches Institut, Universität Stuttgart, Stuttgart, Germany*

²*Jozef Stefan Institute, Jamova 39, 1000 Ljubljana, Slovenia*

³*Max-Planck-Institut für Metallforschung, Stuttgart, Germany*

⁴*Institut für Chemie, Karl-Franzens-Universität, Graz, Austria*

(Dated: August 25, 2021)

Digital video-microscopy measurements are reported of both elastic bandstructures and overdamped phonon decay times in two-dimensional colloidal crystals. Both quantities together allow to determine the friction coefficients along various high symmetry directions in \vec{q} -space. These coefficients contain valuable information on the hydrodynamic forces acting between the colloidal particles. We find Stokes-like friction for phonons near the edge of the first Brillouin zone and vanishing friction coefficients for long wavelength phonons. The effect of this wavelength dependence in real-space is further investigated by simulating a crystal with constant friction (Langevin simulation) and comparing experimentally measured and simulated particle auto-correlation functions.

I. INTRODUCTION

The lattice dynamics of crystals composed of colloidal particles is entirely different from that of atoms. Being immersed in a viscous solvent, colloids experience friction which strongly dampens their motion. As a result, phonons in colloidal systems – characterized by the polarization index j and the wave-vector \vec{q} – show an overdamped dynamics and decay exponentially with decay times $T(\vec{q}j)$. These times are related to the eigenvalues $\lambda(\vec{q}j)$ of the dynamical matrix which are referred to as the elastic bandstructure in the following. These eigenvalues may be pictured as the “spring-constant” associated with the phonon ($\vec{q}j$). In overdamped systems, the relation between $T(\vec{q}j)$ and $\lambda(\vec{q}j)$ is the phonon dispersion curve which replaces the relation between the frequency of the propagating phonons and the bandstructure $\lambda(\vec{q}j)$ in atomic systems. The phonon dispersion curve quantifies the response of a crystal to perturbations of a given wavelength; as such it is *the* central relation of every crystal, characterizing both its static and dynamical properties.

Contrary to atomic systems, where the phonon dispersion curve is entirely determined by interparticle forces, in colloidal systems hydrodynamic interactions have to be considered. These interactions arise when moving colloids exchange momentum through the solvent. Because of their long-ranged nature these interactions are difficult to treat theoretically, especially in crystals [1]. It has been demonstrated by Hurd et al. [2, 3] that along certain high symmetry directions within the colloidal crystal hydrodynamic interactions can be taken into account through the wavelength dependence of the friction coefficients $\gamma(\vec{q}j)$. These coefficients connect the phonon decay times and the bandstructure such that in the limit of strong damping ($\gamma(\vec{q}j) \gg \lambda(\vec{q}j)$) the phonon dispersion relation becomes $T(\vec{q}j) = \gamma(\vec{q}j)/\lambda(\vec{q}j)$. Hence, with the wavelength dependence of the friction coefficients one obtains detailed information also on the hydrodynamic

forces acting within colloidal crystals.

The purpose of this paper is to report measurements of colloidal crystal dispersion curves of thermally excited overdamped phonons, and, more specifically, measurements of the \vec{q} -dependence of the friction coefficients involved. We will compare the experimental data with Langevin simulations where the friction is taken into account only by the constant Stokes friction. This comparison will demonstrate what effect the wavelength dependence of the friction can have on correlations in real space. The simulations also serve to check for the consistency of the evaluation procedure, for finite size effects as well as possible sampling errors.

Measuring \vec{q} -dependent friction coefficients in colloidal crystals is experimentally demanding, and such experiments have – to our knowledge – never been attempted. Such studies require the simultaneous measurement of both the decay times and the bandstructure. While decay times are experimentally accessible with dynamic light scattering techniques [2, 4, 5, 6, 7] or Brillouin scattering [8, 9], the experimental determination of $\lambda(\vec{q}j)$ requires real space positional information. Due to the mesoscopic time- and length scales, such information is accessible in colloidal systems with digital video microscopy which allows to follow particle positions with a resolution of a few nm at video rates as high as 25 Hz.

The literature on phonon dynamics in overdamped systems is still manageable. Of central importance to the present paper is the work of Hurd et al. [2] who starting from [1] not only present a theory of hydrodynamic interaction in colloidal crystals but also performed photon-correlation spectroscopy measurements to study the dispersion of lattice waves. Early studies of single-particle dynamics within colloidal crystals employed scattering techniques [10, 11], while the first video-microscopy experiments relevant for our question were presented by Bongers and Versmold [12] who measured the particle mean square displacement as a function of time, later theoretically analysed within the framework of the Langevin

model in [13, 14].

Hydrodynamics within colloidal systems that are not in the crystalline state, is the subject of a large number of papers. Digital video microscopy has been used to investigate dynamic properties (dynamic structure factor, the hydrodynamic function, hydrodynamic diffusion coefficients) in colloidal suspensions confined between two parallel glass plates [15, 16, 17]. Colloidal friction has also been a major issue in recent optical tweezer measurements of the hydrodynamic interaction between two colloidal particles [18, 19, 20]. The time-independent hydrodynamic forces as well as the cross-correlation function of the colloid position have been interpreted in terms of two-body hydrodynamic interactions, embodied by the Oseen tensor. However, a two-body description of hydrodynamics in crystals is inadequate because of the neglect of many-body effects which dominate the hydrodynamic interaction in regular arrays of particles [1, 2].

When at long wavelengths the frictional force vanishes, damping can become so weak that even in colloidal systems phonons should be able to propagate. Hurd et al. predicted a switch to such propagating modes for transverse modes but were not able to observe them, probably because of the finite-cell geometry and hydrodynamic wall effects – a conclusion that has later been corroborated by Derksen et al. [4] who carefully reconsidered the Hurd experiment. An alternative explanation offered by Felderhof and Jones [21] in terms of additional damping through retarded counterions was challenged by Derksen et al. [4] and Hoppenbrouwers et al. [5]. Evidence for overdamped transverse modes turning propagative at long wavelengths has later been produced by Tata et al. [7] in finite size millimeter crystals. We here completely ignore such propagating modes, returning to a brief discussion of their possible existence only in the last section.

The paper starts with a short presentation of the overdamped Langevin model of a colloidal crystal, which forms the basis of our simulations. Then, the experimental setup is described, followed by a section in which we outline how bandstructures, friction coefficients and correlation functions are obtained from particle configurations. We proceed with the coefficients and the particle auto-correlation functions to show the differences between systems with and without wavelength-dependent friction, i.e., the differences between simulation and experiment. The main conclusions of the paper are formulated in the last section.

II. EXPERIMENTAL

A. Simulation: The overdamped Langevin model of a colloidal crystal

We consider a two-dimensional (2D) hexagonal crystal of N colloidal spheres with diameter σ immersed in an aqueous electrolyte being characterized by the dielectric constant ϵ and the inverse screening length κ . Particle

positions at time t are denoted by $\vec{x}_n(t)$ with n labeling a hexagonal lattice site \vec{R}_n . The position vector decomposes into $\vec{x}_n(t) = \vec{R}_n + \vec{u}_n(t)$ with $\vec{u}_n(t)$ being the particle displacement from the lattice site \vec{R}_n . The interaction of two colloids at distance r is given by the Yukawa potential,

$$\Phi(r) = \frac{(Z_{eff}e)^2}{4\pi\epsilon_0\epsilon} \frac{\exp(\kappa\sigma)}{(1 + \kappa\sigma/2)^2} \frac{\exp(-\kappa r)}{r} \quad (1)$$

where Z_{eff} is the effective colloidal charge. Within the framework of the harmonic approximation, the particles interact through elastic forces characterized by the spring constant k_0 , given by

$$k_0 := \left[\frac{d^2\Phi(r)}{dr^2} - \frac{1}{r} \frac{d\Phi(r)}{dr} \right]_{r=a} \quad (2)$$

where a is the nearest-neighbor distance in the hexagonal crystal.

As explained in the next section, in our experiments the colloidal crystal is stabilized by a commensurate hexagonal, light-induced substrate created by three interfering laser beams. In the sample plane, the electric fields of the linearly polarized laser beams are given by

$$\vec{E}_j(\vec{x}) = \vec{A}_0 \exp(i\vec{K}_j\vec{x}) \quad j = 1, 2, 3 \quad (3)$$

$$\text{with } \vec{K}_1 = Ka\vec{e}_y,$$

$$\vec{K}_2 = K \left(-\frac{\sqrt{3}}{2}a\vec{e}_x - \frac{a}{2}\vec{e}_y \right),$$

$$\vec{K}_3 = K \left(\frac{\sqrt{3}}{2}a\vec{e}_x - \frac{a}{2}\vec{e}_y \right)$$

where $\vec{e}_x = [1, 0]$ and $\vec{e}_y = [0, 1]$ are the basis vectors of Cartesian coordinates, and K is chosen to match commensurate conditions. The interfering laser beams create the substrate potential

$$\begin{aligned} \Phi_{ext}(\vec{x}) &= \frac{A_0^2}{2} \left(9 - \left| \sum_{i=1}^3 \exp(i\vec{K}_i\vec{x}) \right|^2 \right) \\ &= A_0^2 \left(3 - \sum_{i<j} \cos[\vec{K}_{ij}\vec{x}] \right) \end{aligned} \quad (4)$$

where all three vectors $\vec{K}_{ij} = \vec{K}_i - \vec{K}_j$ must have a length $K' = 4\pi/(\sqrt{3}a)$ to ensure a fully commensurate substrate. To adapt this potential to the harmonic approximation used in our simulations, we expanded the cosine function in eq. (4) for positions $\vec{x}_n = \vec{R}_n + \vec{u}_n$ near a lattice site \vec{R}_n , and finally obtain

$$\Phi_{ext}(\vec{R}_n + \vec{u}_n) \approx \frac{A_0^2 K'^2}{2} \sum_{i<j} [\vec{K}'_{ij}\vec{u}_n]^2 \quad (5)$$

where $\vec{K}'_{ij} = \vec{K}_{ij}/K'$ and where use was made of $\vec{K}_{ij} \cdot \vec{R}_n = 2\pi m$ with an integer m . Thus, we arrive at another

spring constant

$$k_1 := A_0^2 K'^2 = \left(\frac{A_0 4\pi}{\sqrt{3}a} \right)^2 \quad (6)$$

defining the strength of the springs with which every particle is pinned to its lattice site \vec{R}_n .

Having introduced k_0 and k_1 we can now proceed to the model equation describing the dynamics of the colloidal crystal. We here adopt a simplified Langevin description of the lattice dynamics, ignore hydrodynamic interactions and include just the Stokes friction between the colloids and the solvent. For more elaborate lattice dynamic theories for colloidal crystals including hydrodynamic interactions, see [2, 21, 22, 23, 24].

If \vec{R}_n is an arbitrary reference site of the hexagonal lattice with its six nearest neighbors $\vec{R}_1 = \vec{R}_n + a\vec{e}_y$, $\vec{R}_2 = \vec{R}_n - \sqrt{3}a/2\vec{e}_x + a/2\vec{e}_y$, and so forth, the overdamped Langevin equation in the harmonic approximation reads

$$\begin{aligned} & \gamma \frac{\partial u_{n\alpha}(t)}{\partial t} \\ & + \frac{k_0}{a^2} \sum_{m=1}^6 \sum_{\beta=x,y} (R_{m\alpha} - R_{n\alpha})(R_{m\beta} - R_{n\beta}) \\ & \times [u_m(t) - u_n(t)] + k_1 u_{n\alpha}(t) + f_{n\alpha}(t) = 0. \end{aligned} \quad (7)$$

where we have restricted ourselves to nearest-neighbor interactions and where an insignificant term $\sim \delta_{\alpha\beta} \Phi'(r)/r$ has been omitted. $\vec{f}_n(t)$ is a randomly fluctuating force for which the following thermal averages must be satisfied

$$\begin{aligned} \langle f_{n\alpha}(t) \rangle &= 0, \\ \langle f_{n\alpha}(t) f_{n'\alpha'}(t + \tau) \rangle &= 2\gamma k_B T \delta(\tau) \delta_{nn'} \delta_{\alpha\alpha'} \end{aligned} \quad (8)$$

with $k_B T$ being the thermal energy. In eq. (7), we have introduced the Stokes friction coefficient γ which measures how strongly a quiescent fluid resists the motion of an isolated sphere. Clearly, this is a rough approximation as the results of the present paper will once more confirm: neither can a crystal particle be considered isolated, nor is the surrounding fluid quiescent, but will in fact be itself in a dynamical state due to the motion of all other particles.

One can express the times in units of $\gamma \mu\text{m}^2/k_B T$ and the spring constant k_0 in terms of $k_B T/\mu\text{m}^2$ such that the number of independent input parameters to eq. (7) is reduced to just three values. In our simulations we have chosen $k_0 \mu\text{m}^2/k_B T = 20$, $k_1/k_0 = 0.6$ and $a = 4 \mu\text{m}$. While the simulations have been performed with reduced units, the data will be presented in normal physical units.

Finally, it must be mentioned that for technical reasons a value of $k_0 \mu\text{m}^2/k_B T = 20$ and above turned out to be the most convenient choice. These values are well above the ones observed in our experiments; however, the band structure scales with k_0 as has been shown in [25] and, therefore, our simulations allow for a meaningful analysis of the experimental results.

B. Experiment: 2D colloidal crystals stabilized by light-induced substrates

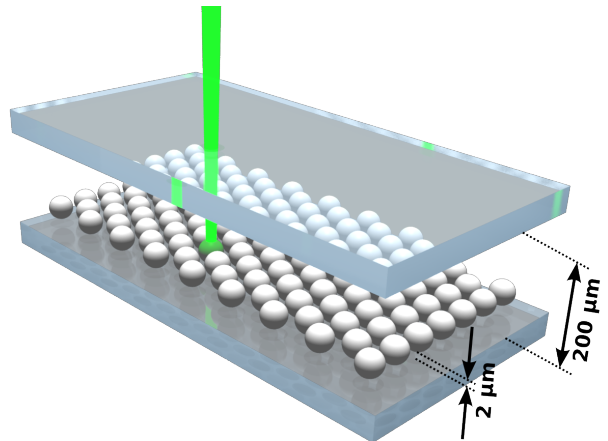


FIG. 1: Sketch of the sample cell containing the 2D crystal subject to a light-induced substrate (indicated for one particle) and, additionally, pressed down towards the bottom plate by a normal incident laser beam.

Experiments were performed with an aqueous suspension of highly charged polystyrene spheres with $\sigma = 2.4 \mu\text{m}$ diameter and a polydispersity below 4%. The particles interact via a screened Coulomb potential, eq. (1), with a renormalized surface charge of about $Z_{eff} \approx 14000$ [26] and a screening length $\kappa^{-1} \approx 458 \text{ nm}$, determined as described further below. As sample cell we used a cuvette made of fused silica with $200 \mu\text{m}$ spacing between top and bottom plate which was connected to a standard closed deionization circuit to maintain stable ionic conditions during the measurements. An Argon-ion laser beam (wave length = 488 nm) was scanned around the central region of the sample to create a boundary box whose size could be continuously adjusted by a pair of computer-controlled galvanostatically driven mirrors. This allowed us to adjust precisely the particle area density [27]. At sufficiently high particle densities the particles form a hexagonal 2D colloidal crystal ($a = 6 \mu\text{m}$) close to the bottom plate (see Fig. 1). Out-of-plane fluctuations are reduced by pushing the particles down towards the bottom plate with a normal incident laser beam. Due to the interplay of the electrostatic particle-wall repulsion and the light pressure from above, this results in a mean particle-wall distance of about $2 \mu\text{m}$ and normal fluctuations of an amplitude of less than 100 nm . By systematic variation of the light pressure we have verified that within our parameters it does not influence the results discussed below.

It is known that 2D crystals cannot have perfect long-ranged translational order because low- \vec{q} phonons destabilize the system. This would considerably reduce the

quality of our measured particle configurations and the correlation functions generated from it. We therefore stabilized the crystal by exposing it to the perfectly hexagonal commensurate substrate potential from eq. (4) being created from the interference of the three laser beams in eq. (3) ($P = 5$ W, frequency-doubled Nd:YVO4 laser, wavelength = 532 nm). It has been shown theoretically and experimentally [25, 26] that if the light-induced substrate is created from laser beams of the same intensity the resulting bandstructure is identical to that of the free crystal, except that it is shifted by k_1 .

Particle positions and trajectories were determined for a 16 shell hexagonal crystallite ($N = 817$ particles) which was part of a much larger crystal comprising about 2000 to 3000 particles. All derived quantities were computed from averages over 29500 images, using digital video microscopy at an acquisition rate of 8 frames per second.

C. Data processing: from configurations to derived quantities

Simulation and experiment produce the same output: sets of particle configurations. These will then be further processed to generate what may be called “derived quantities”. Both sets of configurations, the computer-generated ones as well as the experimental ones, will be processed in the same way.

It is a straightforward procedure to compute for a given configuration the normal coordinates $Q(\vec{q}j, t)$ directly from the measured displacements $\vec{u}_n(t)$ [25]. Here, \vec{q} is one of the N allowed phonon wave vectors, while j is the branch index, $j = 1, 2$, distinguishing between the longitudinal and transversal branch. The normal coordinates allow us to determine the normal mode bandstructure $\lambda(\vec{q}j)$ through the relation

$$A(\vec{q}j) = \langle Q^*(\vec{q}j)Q(\vec{q}j) \rangle = \frac{k_B T}{\lambda(\vec{q}j)}. \quad (9)$$

Several experimental bandstructures of colloidal systems being based on this relation can be found in literature [28, 29, 30]. Starting from the overdamped Langevin equation (7), one finds that the normal-mode auto-correlation function decays exponentially [2, 25],

$$\langle Q^*(\vec{q}j, t + \tau)Q(\vec{q}j, t) \rangle = A(\vec{q}j) \exp\left(-\frac{\tau}{T(\vec{q}j)}\right) \quad (10)$$

with the overdamped phonon dispersion relation

$$T(\vec{q}j) = \frac{\gamma}{\lambda(\vec{q}j)} \quad (11)$$

connecting the phonon decay times $T(\vec{q}j)$ with the elastic bandstructure $\lambda(\vec{q}j)$. So far, the friction coefficient γ has been taken to be constant, relying on the assumption of the Langevin model. Going beyond this model, this latter equation takes a different form. Hurd et al. [2] showed

that along certain high symmetry directions (path sections 1 and 3, see central graph in top row in Fig. 2), hydrodynamic interactions lead to an overdamped phonon dispersion relation of the more general form,

$$T(\vec{q}j) = \frac{\gamma(\vec{q}j)}{\lambda(\vec{q}j)}. \quad (12)$$

where the friction coefficient $\gamma(\vec{q}j)$ is no longer constant, but depends on the band index and the wave vector \vec{q} .

Having introduced these equations, we can formulate more precisely the central idea of the present work. Equation (9) allows us to determine the bandstructure by taking $\lambda(\vec{q}j) = k_B T / A(\vec{q}j)$. Equation (10), on the other hand, permits an independent determination of the decay times $T(\vec{q}j)$. Multiplication of both quantities according to eq. (12) gives us access to the wave-vector dependent friction coefficients,

$$\gamma(\vec{q}j) = \lambda(\vec{q}j)T(\vec{q}j) \quad (13)$$

allowing a detailed experimental study of $\gamma(\vec{q}j)$ and thus also a check of the Langevin model and its assumption of constant friction.

The colloidal crystal dynamics can also be studied by examining the behavior of the particle auto-correlation function

$$\begin{aligned} c(\tau) &= \frac{1}{N} \sum_{n,\alpha} \langle u_{n\alpha}(t + \tau)u_{n\alpha}(t) \rangle \\ &= \frac{1}{N} \sum_{\vec{q},j} \langle Q(\vec{q}j, t + \tau)Q^*(\vec{q}j, t) \rangle, \end{aligned} \quad (14)$$

which is connected to the time-dependent mean-square displacement $\delta_{\text{MSD}}(\tau)$ through

$$c(\tau) = \frac{1}{2}(\delta_{\text{MSD}}(\infty) - \delta_{\text{MSD}}(\tau)). \quad (15)$$

Within the Langevin description, this auto-correlation function is related to the Laplace transform of the phonon spectrum [25]

$$\frac{k_0 c(\tau')}{k_B T} = 2 \int d\lambda' \frac{G(\lambda')}{\lambda'} \exp(-\lambda' \tau') \quad (16)$$

where $\tau' = \tau k_0 / \gamma$, $\lambda' = \lambda / k_0$ and where

$$G(\lambda) = \frac{1}{2N} \sum_{\vec{q}j} \delta(\lambda - \lambda(\vec{q}j)), \quad (17)$$

is the phonon spectrum, counting the number of $\lambda(\vec{q}j)$ within the interval $[\lambda, \lambda + d\lambda]$. This relation takes a static quantity – the system $\lambda(\vec{q}j)$ of \vec{q} -dependent spring constants – to predict a quantity $c(\tau)$ that characterizes the dynamics of the system. In classical atomic crystals, a similar relation exists, connecting the Fourier transform of the velocity auto-correlation function with the phonon density of states [31]. Equation (16) is, of course, valid only within the framework of the Langevin model.

III. RESULTS

A. bandstructure, phonon decay and friction factors

Figure 2 shows phonon auto-correlation functions computed either from simulation data (left column of plots) or from experimental configurations (right column of plots) for four different allowed wave vectors \vec{q} in the first Brillouin zone (center column of plots). As outlined in eqs. (10) to (13), we expect an exponential decay and therefore fitted the data to the function $A \exp(-\tau/T)$. While such an exponential decay is indeed observed in the Langevin simulation data the experimental data show some deviations at larger times. The experimental and simulation curves are obtained from averages over 29500 and 10000 configurations, respectively. Averaging over time windows of different lengths, one can show that for correlation functions near to the edge of the first Brillouin zone (BZ) these deviations of the experimental curves are due to insufficient sampling. However, for correlation functions near the center of the first BZ, one finds deviations which seem to be independent of the average procedure. This might suggest that these (rather small) deviations are fingerprints of propagating modes which are not considered in our overdamped Langevin description and can thus not be reproduced with exponential fit functions. Such propagating modes are expected when the system is damped, but not overdamped, i.e., when the damping is not strong enough to prevent an oscillatory behavior. The alternative explanation – that these deviations result from the typical 2D instability against low \vec{q} phonons – can be safely ruled out because the system is pinned to a hexagonal lattice by the light-induced substrate.

Performing such fits for all allowed wave vectors along the irreducible path 1 to 3 (see top row in Fig. 2), one obtains the function $T(\vec{q}j)$, that is, the phonon decay times for both branches as a function of the wave vector. These times are plotted in the central row of Fig. 3, for both the experimental as well as the simulation data. On the other hand, one can use equation (9) to determine the elastic bandstructure, plotted for both sets of data in the top row of Fig. 3. Harmonic lattice theory of 2D colloids in light-induced potentials [25] provides us with explicit expressions for the bandstructure; they are fitted in Fig. 3 to the measured structure us-

	path	A	B	C	D
longitudinal	3	0	7.17	-1.45	0.07
longitudinal	1	0	6.72	-1.24	0.07
transversal	3	1.7	1.16	0.28	-0.02
transversal	1	1.7	1.28	0.29	-0.09

TABLE I: Fit-parameters of the function $f(x) = A + Bx + Cx^2 + Dx^3$ used in Fig. 4.

ing k_0 and k_1 as fitting parameters. For the bandstructures produced from the simulated data, we obtain $k_1/k_0 = 0.49$ and $k_0 = 18.9 k_B T / \mu\text{m}^2$ in good agreement with the values actually used in the simulation, while from the experimental structures we derive $k_1/k_0 = 0.61$ and $k_0 = 3.3 k_B T / \mu\text{m}^2$. With that we can estimate with eq. (2) (assuming $Z_{eff} = 14000$) a value for $1/\kappa$ of 458 nm which is actually quite a reasonable value. As expected, due to the presence of the stabilizing substrate the bandstructures are slightly shifted upwards, with a shift that is directly proportional to the constant k_1 .

Following eq. (13) we multiply the two quantities $\lambda(\vec{q}j)$ and $T(\vec{q}j)$ to obtain the friction coefficients $\gamma(\vec{q}j)$, plotted in the bottom row of Fig. 3. In the simulations we used the value $\gamma = 8.33 k_B T \text{s} / \mu\text{m}^2$ and a similar value $\gamma = 8.85 k_B T \text{s} / \mu\text{m}^2$, independent of the wave-vector, comes out from the evaluation procedure. This demonstrates the internal consistency of our scheme and the correct implementation of our data evaluation procedures. More importantly, it shows (i) that our statistics (which in the experiment is even better) is sufficient, and (ii) that finite size effects are negligible. While in the experiment we analysed a 16 shell hexagonal crystallite being part of a much larger crystal, the simulation has been carried out with 1000 particles and analysed within a 12 shell hexagonal crystallite comprising 469 particles. Finite size effects would show up in strong variations of $\gamma(\vec{q}j)$ near the center of the BZ – something we do not observe in Fig. 3. Since the experimental system size is considerably larger than in the simulation, we can be rather confident that also the experimental data are not polluted by finite size effects.

With that we turn to our main result – the function $\gamma(\vec{q}j)$ derived from the experimental data (Fig. 3F). We observe pronounced variations of the friction coefficient, having roughly constant values only in one band and only very close to the edge of the BZ. Most importantly, for both bands $\gamma(\vec{q}j)$ tends to zero for $\vec{q} \rightarrow 0$. Almost the same function $\gamma(\vec{q}j)$ is obtained when the renormalized simulated bandstructure is multiplied with the experimental decay times. This finding demonstrates that it is essentially the differences in $T(\vec{q}j)$ which lead to the differences in $\gamma(\vec{q}j)$ between experiment and simulation. The different $\vec{q} \rightarrow 0$ behavior of the friction coefficients can then be traced back to the decay times in this limit being considerably longer in the simulation than in reality, implying that experimentally the long wavelength phonons are decaying much faster than the Langevin simulation with its constant friction assumption suggests. This is an effect due to hydrodynamic interactions that shall be further discussed in the last section.

Figure 4 shows again the measured friction factors: now the coefficients for both \vec{q} directions, path 1 and 3 (see top row in Fig. 2), appear over the same axis. Also, the coefficients have been averaged over three equivalent directions in \vec{q} -space. Note that consideration of all other directions is obsolete due to symmetry reasons. To facilitate easy reproduction of our results we have fitted the

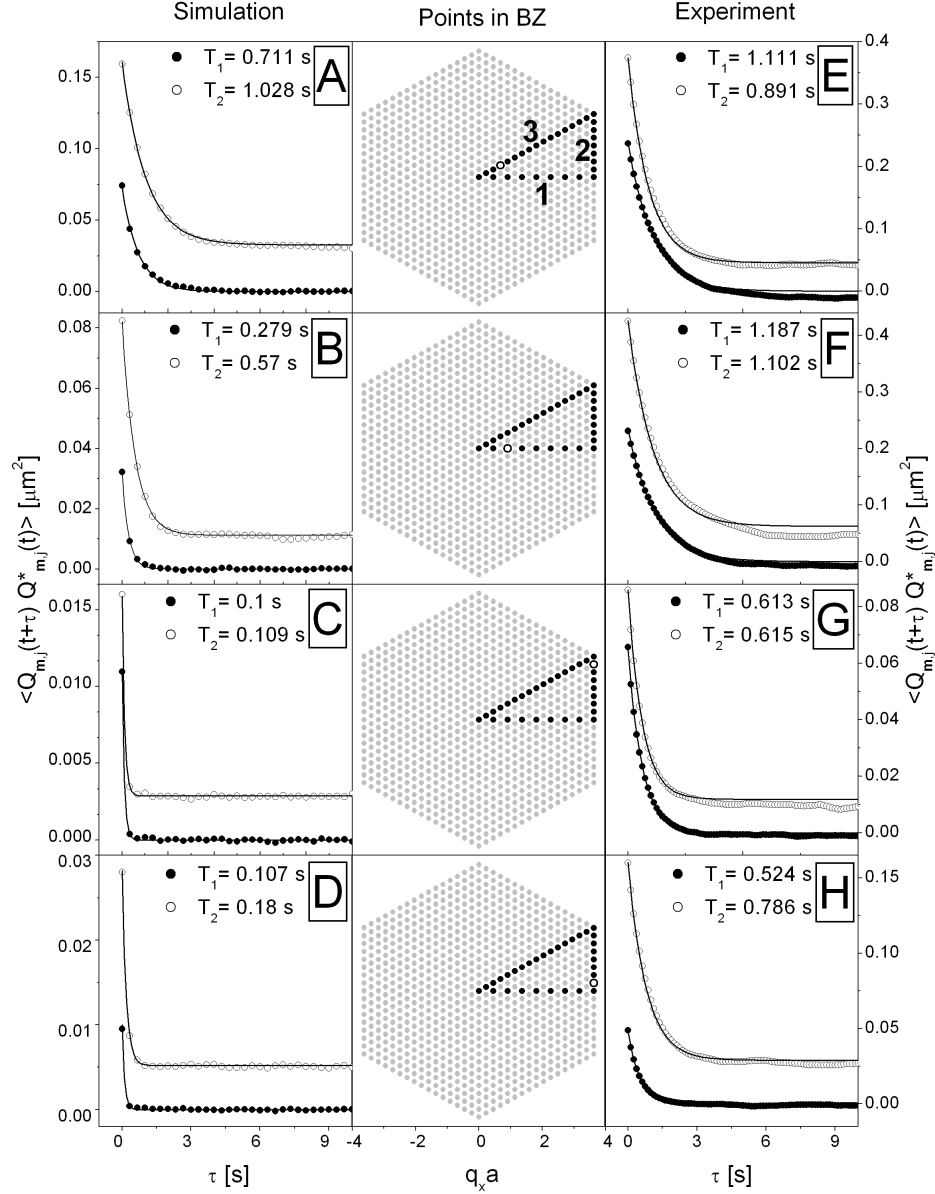


FIG. 2: Phonon auto-correlation function for the two band indices $j = 1$ (closed symbols) and $j = 2$ (open symbols) at certain \vec{q} values in the first Brillouin zone, as determined from Langevin simulation data (A-D) and from video-microscopy data (E-H). The center column shows the 817 allowed phonon wave vectors \vec{q} in the first Brillouin zone; the \vec{q} value actually considered in the respective row is represented as a black open symbol, \vec{q} -vectors along the irreducible path are printed as solid black symbols, gray color is used otherwise. The numbers in the top graph label the sections of the path around the irreducible part of the first Brillouin zone. The solid lines are exponential fits to the data with the resulting phonon decay times given in the legend of each figure. The curves for $j = 2$ (open symbols) are vertically shifted for clarity.

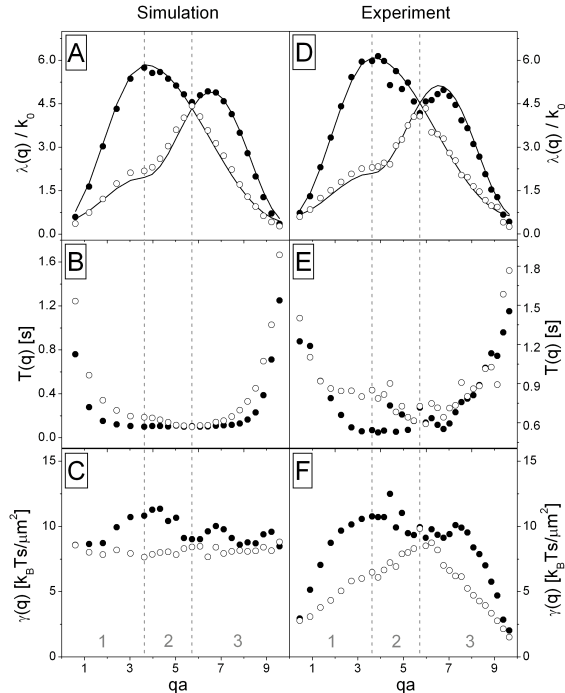


FIG. 3: Elastic bandstructure $\lambda(\vec{q}j)$ (top pair of graphs), phonon decay times $T(\vec{q}j)$ (central pair of graphs), and wavelength-dependent friction coefficient $\gamma(\vec{q}j)$ (bottom row), plotted along the irreducible path 1 to 3 of the first Brillouin zone (see top row in Fig. 2). Solid lines in the upper graph represent bandstructures calculated within the framework of harmonic lattice theory.

curves to a polynomial, with the fitting parameters given in table I. We observe for $q \rightarrow 0$ that while the fitted functions of the longitudinal branches go to zero, those of the two transversal modes extrapolate our results to a value slightly larger than zero. We expect that this extrapolation is not very meaningful as the real curve between $q = 0$ and our first measured data point might be completely different because of the emergence of propagating phonons in this \vec{q} regime which would destroy the basis of our determination of $T(\vec{q}j)$.

We finally observe that the theoretical Stokes friction coefficient $6\pi\eta(\sigma/2)$ for our colloidal spheres in water is $5 k_B Ts / \mu\text{m}^2$, showing that our coefficients are of a reasonable magnitude (see Fig. 3 and Fig. 4). This statement is supported by the observation presented in [32] where γ increases to $8 - 10 k_B Ts / \mu\text{m}^2$ if the colloidal sphere is located approximately $2 \mu\text{m}$ above a wall.

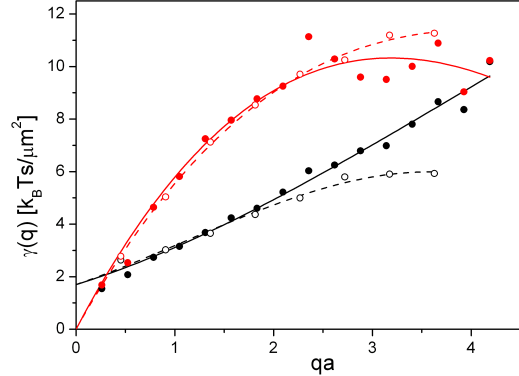


FIG. 4: Measured friction coefficients $\gamma(\vec{q}j)$ as shown in Fig. 3F together with fitted polynomials (lines). Fit parameters are listed in table I. Upper two curves show the coefficients for the longitudinal modes, while the lower two curves correspond to the transversal modes. Open symbols for a direction in \vec{q} -space along path 1 (see top row in Fig. 2), closed symbols for direction along path 3.

B. Phonon spectrum and mean-square displacement

Instead of considering the dynamics of all $2N$ phonons individually, one may also study the colloidal dynamics more globally by examining the average over all *phonon* auto-correlation functions $\langle Q(\vec{q}j, t + \tau) Q^*(\vec{q}j, t) \rangle$, thus arriving at the *particle* auto-correlation function $c(\tau)$ defined in eq. (14). As an average over all phonons, it is perhaps more suited to serve as a general measure of the colloidal dynamics; physically it is directly linked to the time dependent mean-square displacement, eq. (15).

To see how the observed differences between the actual colloid dynamics and the Langevin dynamics manifest itself with respect to the particle auto-correlation function $c(\tau)$, a Langevin prediction of $c(\tau)$ for the experimental system is required. Here, we can exploit the relation (16) which assuming a Langevin system derives a $c(\tau)$ directly from the phonon spectrum $G(\lambda)$ and thus essentially from the bandstructure $\lambda(\vec{q}j)$. A $c(\tau)$ thus predicted can then be confronted with the actual particle auto-correlation function obtained from averaging $\langle u_{n\alpha}(t + \tau) u_{n\alpha}(t) \rangle$ as given in eq. (14). This is the idea of Fig. 5.

The figure shows almost identical phonon spectra for both the simulated and the experimental system. Several singularities can be seen, the most important one is the jump singularity on the left edge of the spectrum. If $k_1 \rightarrow 0$, i.e., if the substrate potential is switched off, this singularity shifts to $\lambda = 0$ and the phonon spectrum $G(\lambda)$ takes a finite value at $\lambda = 0$. This will then lead to a divergent integral in eq. (16) and, as a result, $c(\tau)$ will logarithmically diverge [25]. This is the well-known instability of 2D crystals which we here see to have been

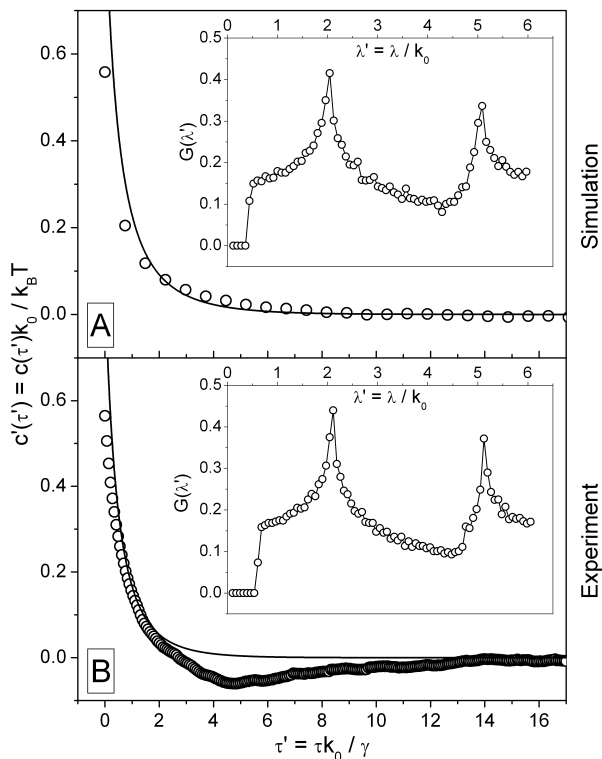


FIG. 5: Insets: phonon spectra, as obtained from applying eq. (17) to the simulated and experimental bandstructures $\lambda(\vec{q}j)$ presented in Fig. 3. Main figures: particle auto-correlation functions obtained from the phonon spectra through a Laplace transformation (solid lines) and by direct evaluation and averaging of $\langle u_{n\alpha}(t+\tau)u_{n\alpha}(t) \rangle$ following eq. (14) (open symbols). A: simulation, B: experiment.

cured thanks to the stabilizing effect of the substrate and the light-induced shift of the jump singularity of $G(\lambda)$ away from $\lambda = 0$.

The Laplace transforms of the phonon spectra, eq. (16), are given as solid lines in the main figures of Fig. 5, and are compared to the $c(\tau)$ obtained from processing particle displacements of 6000 (experiment) and 2000 (simulation) different configurations containing 1017 (experiment) and 563 (simulation) particles. For the simulation, being based exclusively on the Langevin model, we *must* find perfect agreement between both curves, provided our scheme is consistent and the data analysis tools are free from flaws. And, indeed, we do find consistency of the data. As for the experimental system agreement can only be expected as long as the Langevin model applies. We observe a reasonable agreement for the first five seconds (up to $\tau' = 2$) and marked deviations towards negative values between $\tau' = 2$ and

$\tau' = 10$. These deviations are not produced by poor statistics, or by the instability of 2D crystals which we have suppressed by the substrate, but are a real feature of the system. Very likely, it is – in a real-space presentation – the effect of the wave-vector dependence of the friction-coefficients.

IV. DISCUSSION AND CONCLUDING REMARKS

The novel aspect of the present paper is the experimental determination of the wavelength dependence of the friction coefficients in 2D colloidal crystals and, based on these data, a comparison of the colloidal dynamics to the more simplified Langevin dynamics. Determining the \vec{q} -dependence of friction coefficients requires to measure two quantities independently, the elastic bandstructure $\lambda(\vec{q}j)$ and the phonon decay times $T(\vec{q}j)$. The friction coefficients then follow from multiplying both quantities. Such a measurement is possible only with video-microscopy data – a technique whose most appealing property is that it allows us to directly “see” the overdamped dynamics of the colloids, in the form of the exponential decay of the phonon auto-correlation function in Fig. 2.

Our main finding is that in the long-wavelength limit, the friction coefficient vanishes, i.e., $\gamma(\vec{q}j) \rightarrow 0$ for $q \rightarrow 0$. This is clearly the case for the longitudinal modes while the extrapolated curves for the transversal modes show a small offset at $q = 0$ which however is probably not a meaningful extrapolation. The vanishing of friction of long wavelength phonons is a very reasonable result. Hurd et al. pointed out that in 3D colloidal crystals back flow will give an extra damping to longitudinal modes such that for $q \rightarrow 0$ the damping is even larger than the Stokes friction coefficient. Transverse modes, on the other hand, have been shown not to be affected by a back-flow damping; the flow induced by the collective motions of the spheres now adds constructively, leading to vanishing friction coefficients at long wavelengths. Quite the same mechanism can be postulated to work for our 2D system: the transverse modes in the limit $q \rightarrow 0$ will also induce constructive interference of the flow, an overall flow field occurs going in the same direction than the moving colloids and, as a result, the colloidal particle show no longer motion relative to the surrounding fluid, leading to a vanishing of the friction and thus a faster decay of the overdamped phonons. For longitudinal modes, our 2D system differs from the 3D system in that the 2D layer of particles is coupled to a third spatial dimension into which the flow is free to move. This third dimension prevents the back-flow damping, and a favorable interference of the flow into the third dimension should again be the reason for the vanishing of the friction coefficient for $q \rightarrow 0$. However, a more detailed explanation – as well as a theoretical reproduction of $\gamma(\vec{q}j)$ in Fig. 3 – has to wait for a proper hydrodynamic theory describing our system.

Such a theory must also account for hydrodynamic effects resulting from the walls confining our systems [33]. Our results might also be interesting to be reproduced applying more advanced simulation techniques [34] taking into account many-particle hydrodynamics.

With these results in mind, it is clear that taking a constant friction coefficient is a rather gross assumption of the overdamped Langevin model. In addition, this model ignores that vanishing friction coefficients in the long wavelength limit necessarily permits phonons to start propagating (though being still damped, but not overdamped). Systematic deviations from the exponentials in Fig. 2 might be seen as a first indication for the existence of such modes. However, it is also evident from Fig. 2 that given these deviations indeed signalize the onset of propagating phonons, they are still rather weak and far from being able to dominate the overall dynamics of the system. The success and failure of the overdamped Langevin model is best summarized by Fig. 5 showing a particle auto-correlation function $c(\tau)$ that agrees to the Langevin prediction only within the first few seconds. Beyond that time, clear deviations towards negative values in $c(\tau)$ (anti-correlated behavior) can be observed, a feature which according to our previous remarks must be due to the combined effect of the wave-length dependence of the friction coefficient and, possibly, propagating modes. Such a time-delayed anticorrelation has also

been observed in the two-particle experiments and has been interpreted in terms of the standard Oseen tensor hydrodynamic coupling [18]. Zahn et al. also showed that the Oseen term in 2D colloidal suspensions can lead to an increase of the self-diffusion [35]. Again: how these results connect to our findings and how exactly hydrodynamics produces the anticorrelation, can only be clarified with an elaborate hydrodynamical theory. It is our hope that the present paper can stimulate the interest in such theoretical work.

As well as motivating research on hydrodynamics our work might open novel perspectives in studying crystals which exhibit non-overdamped particle dynamics. Such crystals can be already realized using a dusty plasma [36] where the micron-sized dust particles can be observed with videomicroscopy similar to colloidal crystals.

V. ACKNOWLEDGEMENTS

This project received financial support from the Austrian Science Foundation (FWF) under project title P18762. Jure Dobnikar wants to acknowledge the financial support of the Slovene Research Agency under the Grant P1-0055.

-
- [1] H. Hasimoto, *J. Fluid Mech.* **5**, 317 (1959).
 - [2] A.J. Hurd, N.A. Clark, R.C. Mockler, and W.J. Sullivan, *Phys. Rev. A* **26**, 2869 (1982).
 - [3] A.J. Hurd, N.A. Clark, R.C. Mockler, and W.J. Sullivan, *J. Fluid. Mech.* **153**, 401 (1985).
 - [4] J. Derksen and W. van de Water, *Phys. Rev. A* **45**, 5660 (1992).
 - [5] M. Hoppenbrouwers and W. van de Water, *Phys. Rev. Lett.* **80**, 3871 (1998).
 - [6] Z. Cheng, J. Zhu, W.B. Russel, and P.M. Chaikin, *Phys. Rev. Lett.* **85**, 1460 (2000).
 - [7] B.V.R. Tata, P.S. Mohanty, M.C. Valsakumar, and J. Yamanaka, *Phys. Rev. Lett.* **93**, 268303 (2004).
 - [8] R.S. Penciu, M. Kafesaki, G.Fytas, E.N. Economou, W. Steffen, A. Hollingsworth, and W.B. Russel, *Europhys. Lett.* **58**, 699 (2002).
 - [9] R.S. Penciu, H. Kriegs, G. Petekidis, G. Fytas, and E.N. Economou, *J. Chem. Phys.* **118**, 5224 (2003).
 - [10] R. Piazza and V. Degiorgio, *Phys. Rev. Lett.* **67**, 3868 (1991).
 - [11] A. Brands, H. Versmold, and W. van Meegen, *J. Chem. Phys.* **110**, 1283 (1999).
 - [12] J. Bongers and H. Versmold, *J. Chem. Phys.* **104**, 1519 (1996).
 - [13] Y.N. Ohshima and I. Nishio, *J. Chem. Phys.* **114**, 8649 (2001).
 - [14] Y.N. Ohshima, K.E. Hatakeyam, M. Satake, Y. Homma, R. Washidzu, and I. Nishio, *J. Chem. Phys.* **115**, 10945 (2001).
 - [15] M. D. Carbajal-Tinoco, G. Cruz de Leon, and J. L. Arauz-Lara, *Phys. Rev. E* **56**, 6962 (1997).
 - [16] J. Santana-Solano and J. L. Arauz-Lara, *Phys. Rev. Lett.* **87**, 038302 (2001).
 - [17] J. Santana-Solano, A. Ramirez-Saito, and J.L. Arauz-Lara, *Phys. Rev. Lett.* **95**, 198301 (2005).
 - [18] J.C. Meiners and S.R. Quake, *Phys. Rev. Lett.* **82**, 2211 (1999).
 - [19] S. Henderson, S. Mitchell, and P. Bartlett, *Phys. Rev. E* **64**, 061403 (2001).
 - [20] N.K. Metzger, R.F. Marchington, M. Mazilu, R.L. Smith, K. Dholakia, and E.M. Wright, *Phys. Rev. Lett.* **98**, 068102 (2007).
 - [21] B.U. Felderhof and R.B. Jones, *Faraday Discuss. Chem. Soc.* **83**, 69 (1987).
 - [22] B.U. Felderhof and R.B. Jones, *Z. Phys. B* **64**, 393 (1986).
 - [23] P.P.J.M. Schram, A.G. Sitenko, and V.I. Zasenkov, *Physica B* **228**, 197 (1996).
 - [24] J.M.A. Hofman, H.J.H. Clercx, and P.P.J.M. Schram, *Physica A* **268**, 326 (1999).
 - [25] H.H. von Grünberg and J. Baumgartl, *Phys. Rev. E* **75**, 051406 (2007).
 - [26] J. Baumgartl, M. Zvyagolskaya, and C. Bechinger, *Phys. Rev. Lett.* **99**, 205503 (2007).
 - [27] M. Brunner, C. Bechinger, W. Strepp, V. Lobaskin and H.H. von Grünberg, *Europhys. Lett.* **58**, 926 (2002).
 - [28] P. Keim, G. Maret, U. Herz, and H.H. von Grünberg, *Phys. Rev. Lett.* **92**, 215504 (2004).
 - [29] D. Reinke, H. Stark, H. H. von Grünberg, A.B. Schofield, G. Maret, and U. Gasser, *Phys. Rev. Lett.* **98**, 038301

- (2007).
- [30] H. H. von Grünberg, P. Keim, and G. Maret, in *Soft Matter*, edited by G. Gompper and M. Schick (Wiley-VCH, Weinheim, 2007), Vol. 3, Chap. 2, pp. 41–85.
 - [31] J.M. Dickey and A. Paskin, *Phys. Rev.* **188**, 1407 (1969).
 - [32] M.I.M. Feitosa and O.N. Mesquita, *Phys. Rev. A* **44**, 6677 (1991).
 - [33] S. Bhattacharya, J. Blawdziewicz, and E. Wajnryb, *Journal of Fluid Mechanics* **541**, 263 (2005).
 - [34] J. Falck, J. M. Lahtinen, I. Vattulainen, and T. Al-Nissila, *The European Physical Journal E* **13**, 1292 (2004).
 - [35] K. Zahn, J.M. Mendez-Alcaraz, and G. Maret, *Phys. Rev. Lett.* **79**, 175 (1997).
 - [36] S. Nunomura, D. Samsonov, and J. Goree, *Phys. Rev. Lett.* **84**, 5141 (2000).